Electronic Supplementary Information (ESI) for

Water-tuned reversible spin transition with the largest hysteresis loop in 3D Hofmann frameworks pillared by flexible ligands

Zhe Feng,[a] Jiejie Ling,[a] Huijie Song[a] and Dun-Ru Zhu*[a,b]
[a] College of Chemical Engineering, State Key Laboratory of Materials-oriented Chemical Engineering, Nanjing Tech University, 30 Puzhu South Road, Nanjing 211816, P.R. China.
[b] State Key Laboratory of Coordination Chemistry, Nanjing University, 163 Xianlin Avenue, Nanjing 210023, P.R. China
* Correspondence e-mail: zhudr@njtech.edu.cn

Contents

1. The reversible transformation between **1**·4.5H_2O-p and **1**·····S2
2. The FT-IR spectra of **1**·4.5H_2O-c, **1**, **2**·4.5H_2O-c, **2** and rehydrated **1**·4.5H_2O-p and **2**·4.5H_2O-p·····S2
3. The TGA curves of **1**·4.5H_2O-c, **1**, **2**·4.5H_2O-c, **2**, rehydrated **1**·4.5H_2O-p and **2**·4.5H_2O-p·····S3
4. The PXRD patterns of **1**·4.5H_2O-c, **2**·4.5H_2O-c, **1**, **2**, rehydrated **1**·4.5H_2O-p and **2**·4.5H_2O-p·····S4
5. Molecular structures of **1**·4.5H_2O-c and **2**·4.5H_2O-c at 296 and 100 K·····S5
6. Selected bond distances and angles and hydrogen bond interactions for **1**·4.5H_2O-c and **2**·4.5H_2O-c at 296 and 100 K·····S8
7. Second magnetic measurements for the hysteretic SCO behaviors of **1**·4.5H_2O-c and **2**·4.5H_2O-c·····S9
8. Comparison of the spin transition parameters of some representative 3D Hofmann SCO frameworks·····S9

1. The reversible transformation between 1·4.5H_2O-p and 1

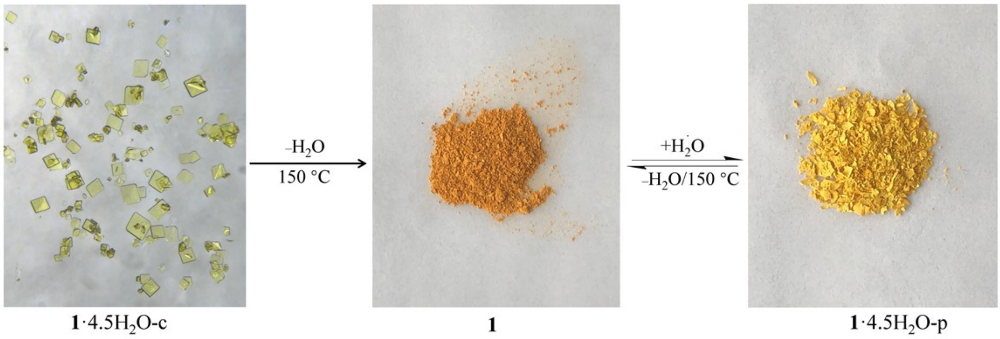

Fig. S1 The reversible transformation between the **1**·4.5H_2O-p and **1**.

2. The FT-IR spectra of 1·4.5H_2O-c, 1, 2·4.5H_2O-c, 2, rehydrated 1·4.5H_2O-p and 2·4.5H_2O-p

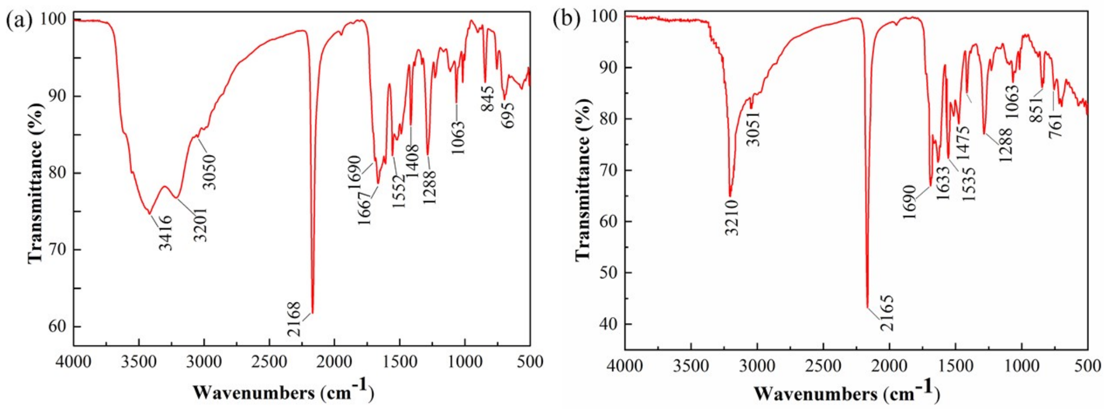

Fig. S2 FT-IR spectra of (a) **1**·4.5H_2O-c and (b) **1**.

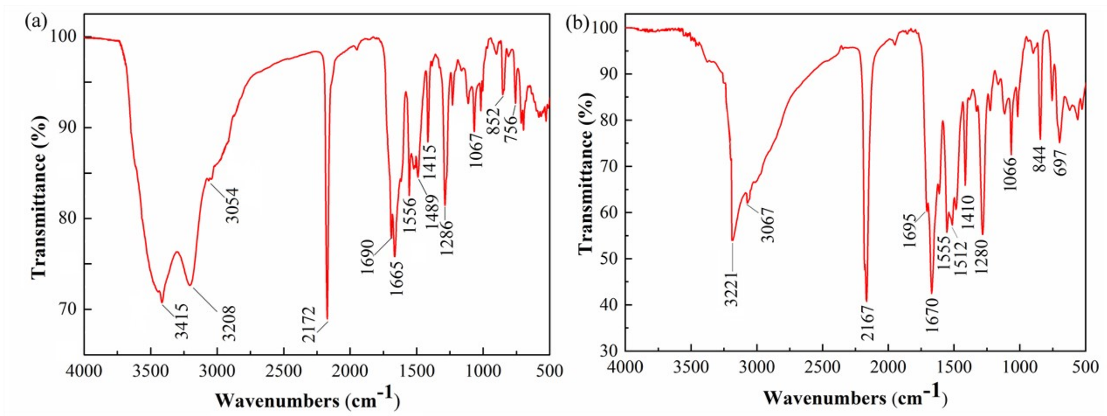

Fig. S3 FT-IR spectra of (a) **2**·4.5H_2O-c and (b) **2**.

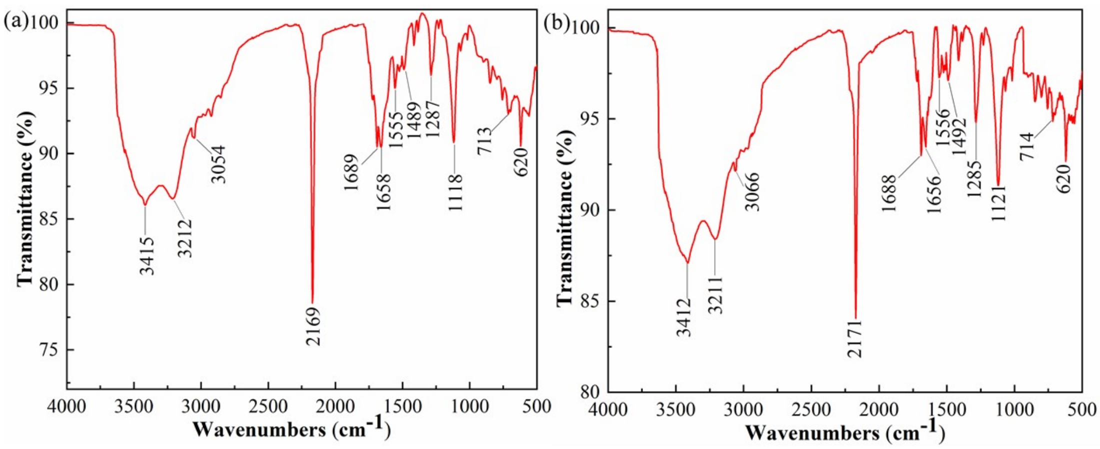

Fig. S4 FT-IR spectra of the rehydrated **1**·4.5H_2O-p (a) and **2**·4.5H_2O-p (b).

3. The TGA curves of 1·4.5H$_2$O-c, 1, 2·4.5H$_2$O-c, 2, rehydrated 1·4.5H$_2$O-p and 2·4.5H$_2$O-p

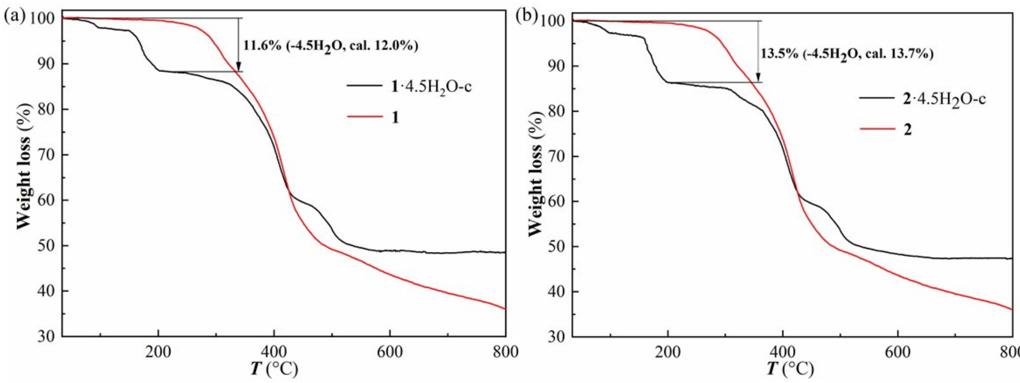

Fig. S5 TGA curves of (a) **1**·4.5H_2O-c and **1** and (b) **2**·4.5H_2O-c and **2**.

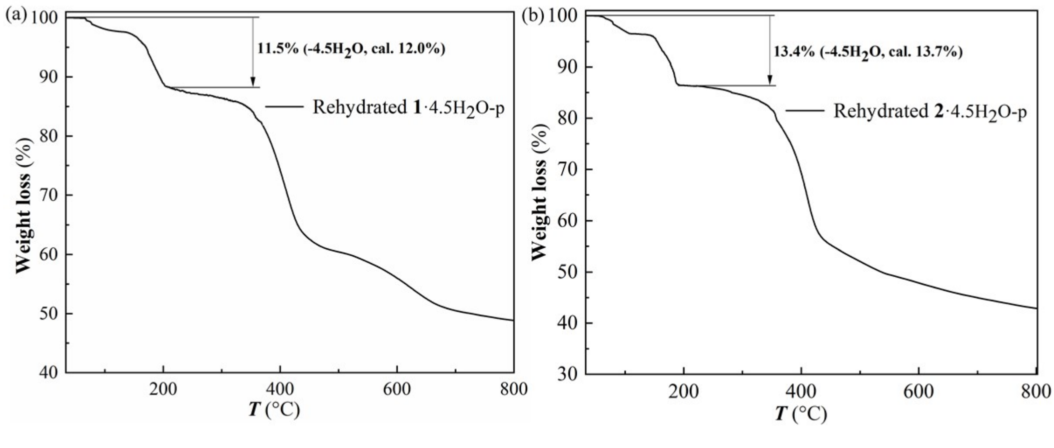

Fig. S6 TGA curves of rehydrated **1**·4.5H_2O-p (a) and **2**·4.5H_2O-p (b).

4. The PXRD patterns of 1·4.5H_2O-c, 2·4.5H_2O-c, 1, 2, rehydrated 1·4.5H_2O-p and 2·4.5H_2O-p

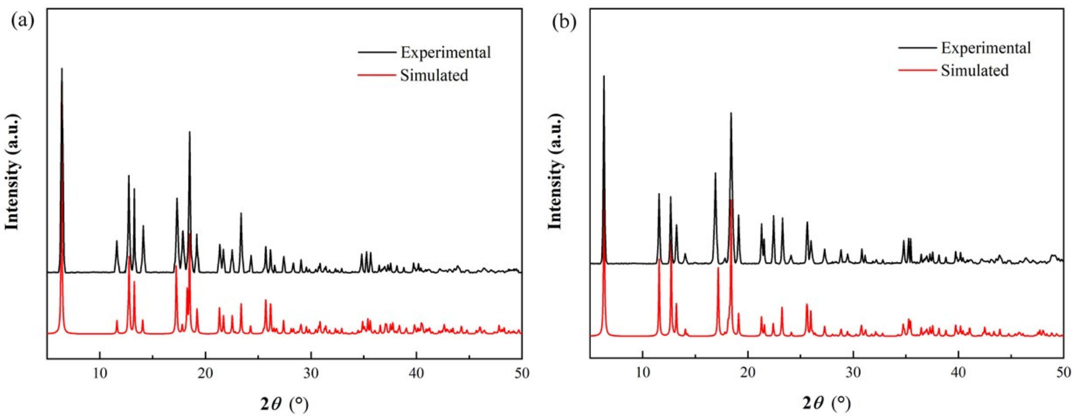

Fig. S7 PXRD patterns of (a) **1**·4.5H_2O-c and (b) **2**·4.5H_2O-c.

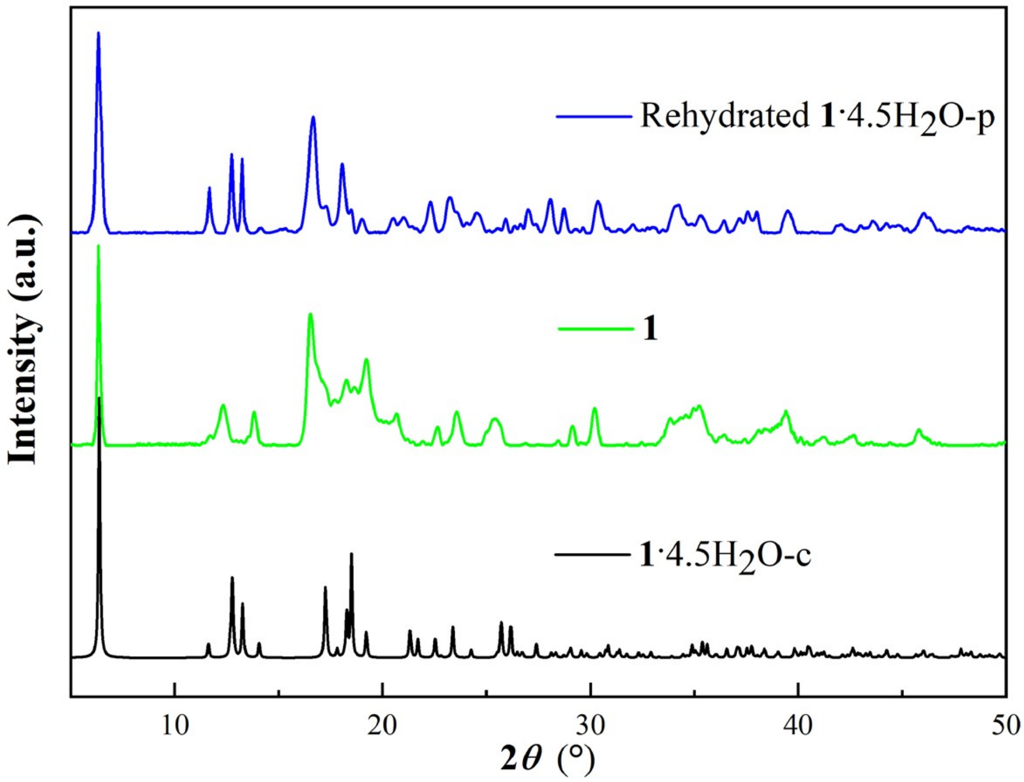

Fig. S8 PXRD patterns of **1**·4.5H_2O-c, **1** and rehydrated **1**·4.5H_2O-p.

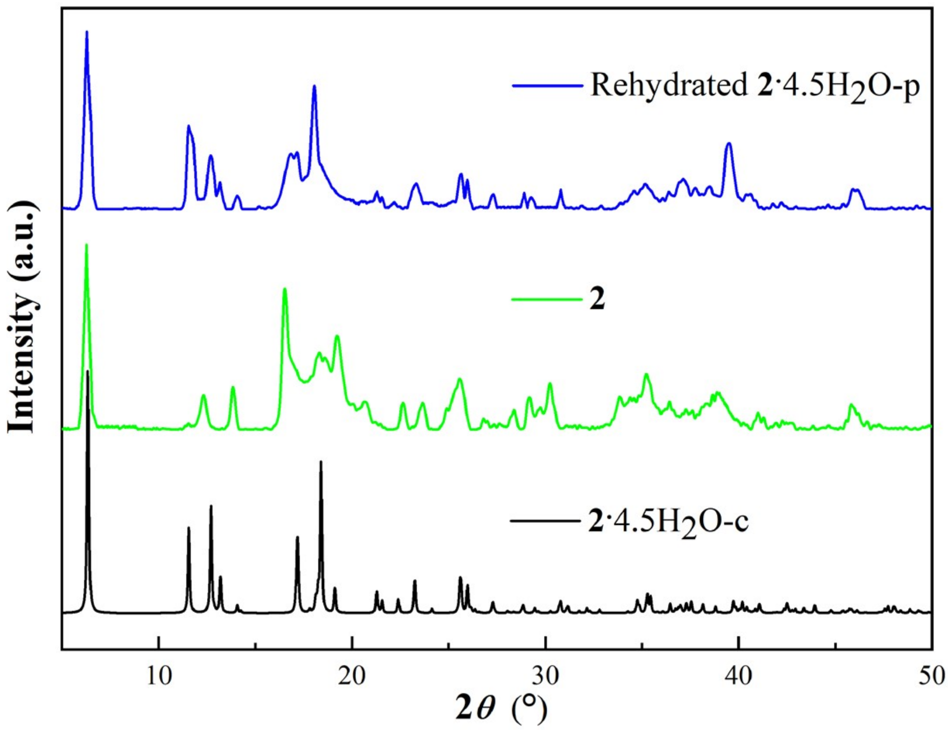

Fig. S9 PXRD patterns of **2**·4.5H_2O-c, **2** and rehydrated **2**·4.5H_2O-p.

5. Molecular structures of 1·4.5H$_2$O-c and 2·4.5H$_2$O-c at 296 and 100 K

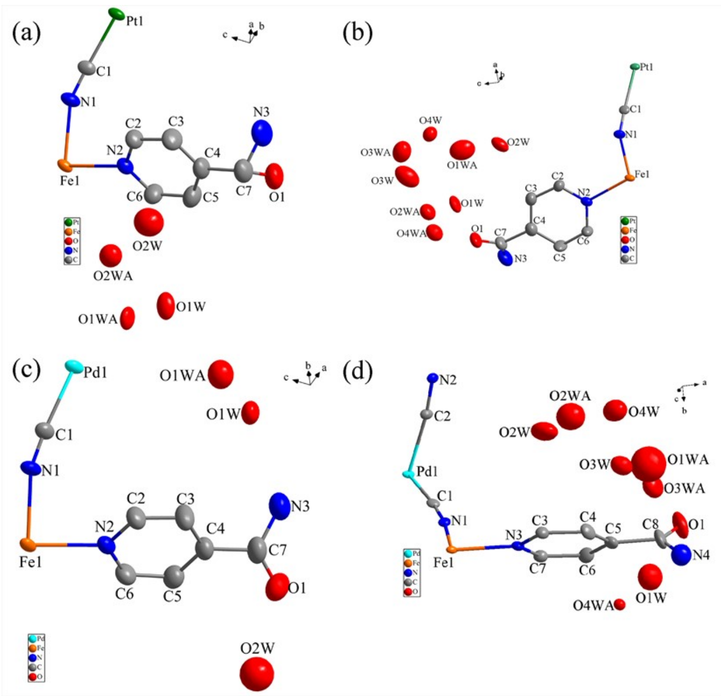

Fig. S10 The asymmetric unit of **1**·4.5H_2O-c at 296 K (a) and 100 K (b), and **2**·4.5H_2O-c at 296 K (c) and 100 K (d) with 50% thermal ellipsoids probability, all hydrogen atoms are omitted for clarity.

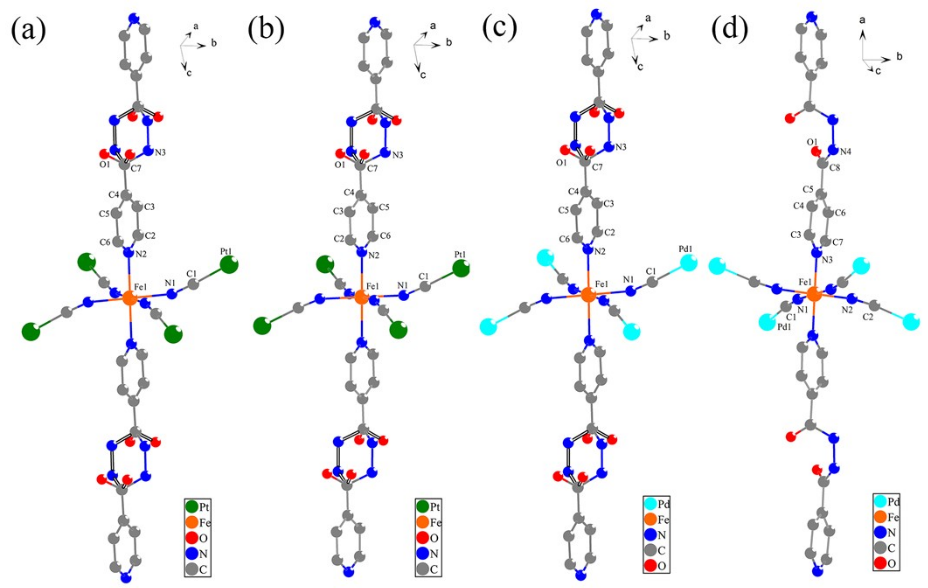

Fig. S11 The coordinated environment of Fe^{2+} ion in **1**·4.5H_2O-c at 296 K (a) and 100 K (b), and **2**·4.5H_2O-c at 296 K (c) and 100 K (d) (the disorder atoms are linked by the hollow lines and all hydrogen atoms are omitted for clarity).

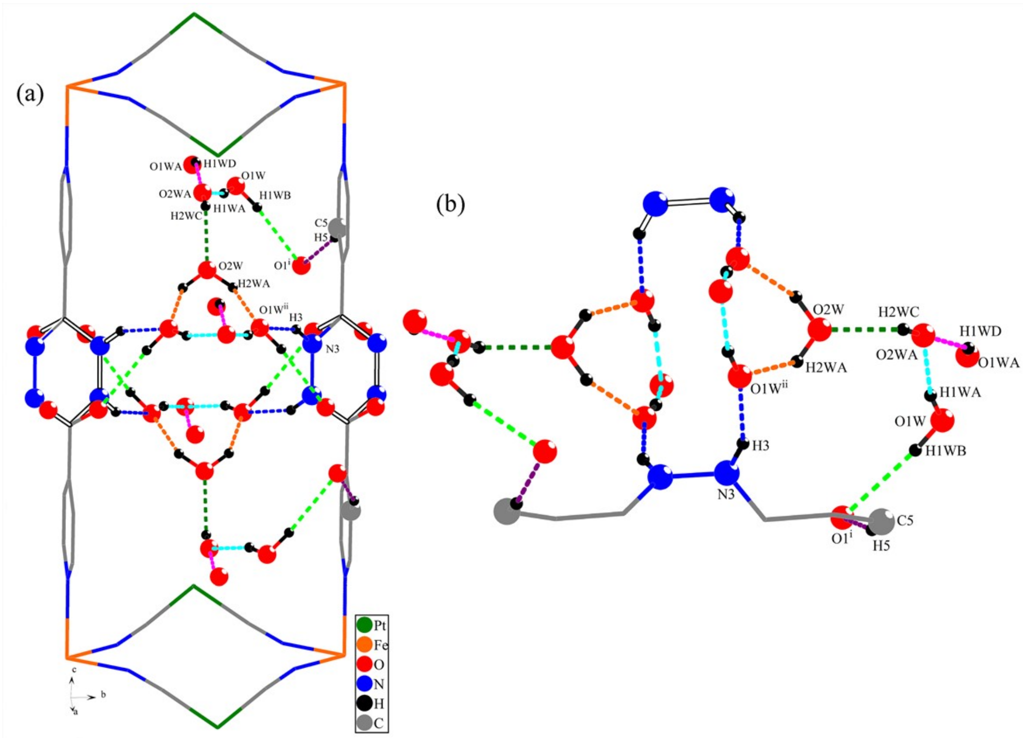

Fig. S12 (a) The hydrogen bond interactions in **1**·4.5H_2O-c at 296 K and (b) the hydrogen-bonding networks formed in the 1D channels of **1**·4.5H_2O-c (the disorder atoms are linked by the hollow lines).

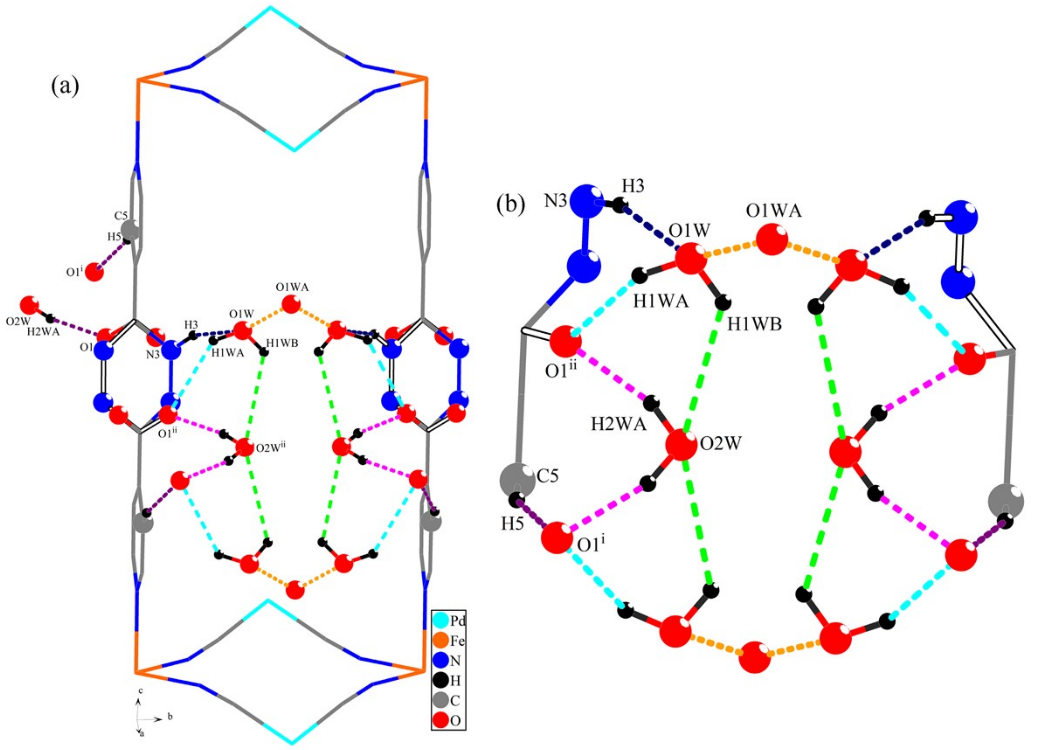

Fig. S13 (a) The hydrogen bond interactions in **2**·4.5H_2O-c at 296 K and (b) the hydrogen-bonding networks formed in the 1D channels of **2**·4.5H_2O-c (the disorder atoms are linked by the hollow lines).

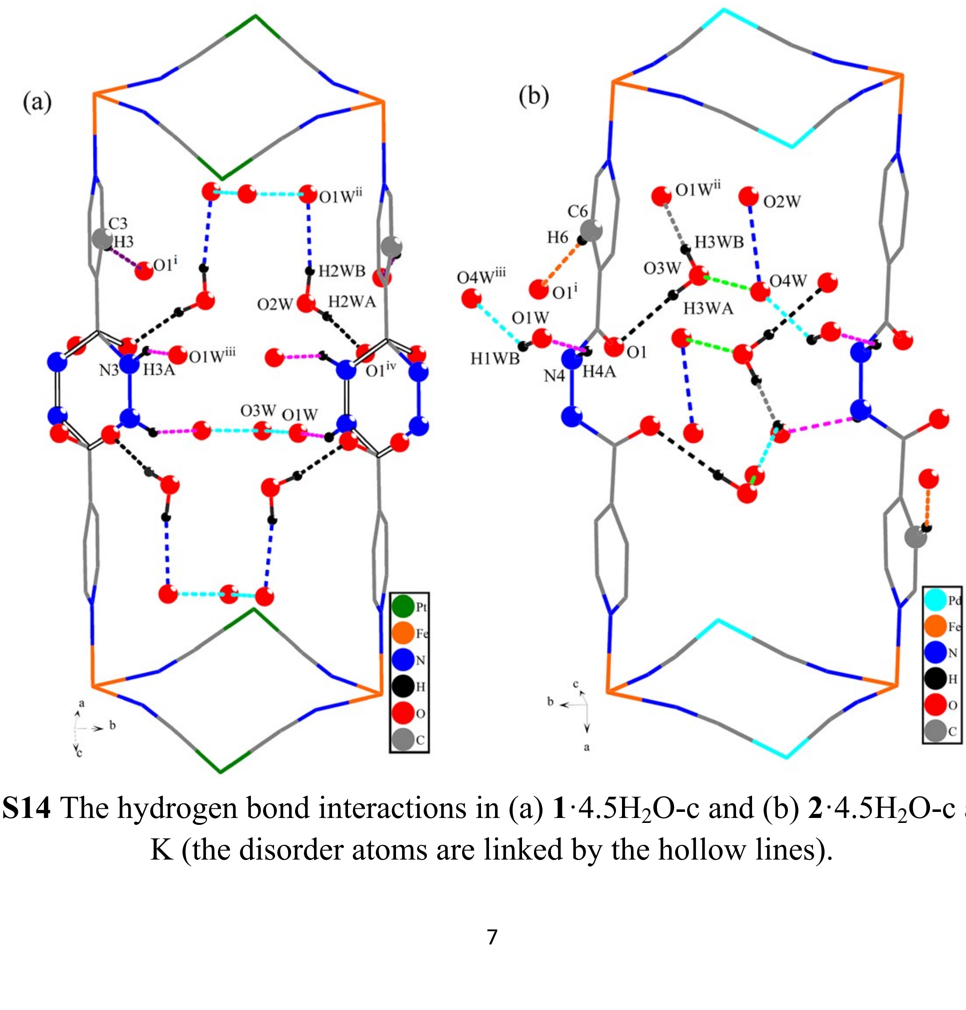

Fig. S14 The hydrogen bond interactions in (a) **1**·4.5H_2O-c and (b) **2**·4.5H_2O-c at 100 K (the disorder atoms are linked by the hollow lines).

6. Selected bond distances and angles and hydrogen bond interactions for **1**·4.5H_2O-c and **2**·4.5H_2O-c at 296 and 100 K

Table S1 Selected bond distances (Å) and angles (°) for **1**·4.5H_2O-c and **2**·4.5H_2O-c at 296 and 100 K

1·4.5H_2O-c				**2**·4.5H_2O-c			
296 K		100 K		296 K		100 K	
Fe1-N1	2.139(4)	Fe1-N1	2.140(4)	Fe1-N1	2.148(3)	Fe1-N1	1.941(4)
						Fe1-N2^{ii}	1.938(4)
Fe1-N2	2.210(6)	Fe1-N2	2.215(5)	Fe1-N2	2.210(4)	Fe1-N3	1.989(4)
Pt1-C1	1.981(5)	Pt1-C1	1.989(5)	Pd1-C1	2.001(4)	Pd1-C1/C2	1.990(5)
C1-N1	1.150(7)	C1-N1	1.144(6)	C1-N1	1.136(5)	C1-N1	1.158(7)
N2-C2	1.330(10)	N2-C2	1.324(9)	N2-C2	1.311(7)	C2-N2	1.160(7)
N2-C6	1.317(11)	N2-C6	1.333(10)	N2-C6	1.347(7)	N3-C7	1.350(7)
C7-N3	1.362(15)	C7-N3	1.403(14)	C7-N3	1.384(11)	C8-N4	1.355(8)
C7-O1	1.177(13)	C7-O1	1.190(12)	C7-O1	1.196(9)	C8-O1	1.206(8)
Fe···Fe^{iii}	10.318(2)	Fe···Fe^{iii}	10.315(2)	Fe···Fe^{iii}	10.361(2)	Fe···Fe^{iii}	10.082(2)
Fe···Fe^{iv}	15.657(2)	Fe···Fe^{iv}	15.679(2)	Fe···Fe^{iv}	15.682(2)	Fe···Fe^{iv}	15.154(2)
N1-Fe1-N2	88.27(16)	N1-Fe1-N2	91.58(15)	N1-Fe1-N2	87.92(12)	N1-Fe1-N3	92.54(16)
N1-Fe1-N2^{i}	91.74(16)	N1-Fe1-N2^{i}	88.42(15)	N1-Fe1-N2^{i}	92.08(12)	N1-Fe1-N3^{i}	88.29(16)
N1-Fe1-N1^{ii}	89.65(2)	N1-Fe1-N1^{ii}	90.85(4)	N1-Fe1-N1^{ii}	88.98(17)	N1-Fe1-N1^{i}	88.3(2)
N1-Fe1-N1^{i}	90.35(2)	N1-Fe1-N1^{i}	89.1(2)	N1-Fe1-N1^{i}	91.02(17)	N1-Fe1-N2^{ii}	91.93(18)
C1-N1-Fe1	157.78(4)	C1-N1-Fe1	157.5(4)	C1-N1-Fe1	159.42(3)	C1-N1-Fe1	168.1(4)
C2-N2-Fe1	122.89(5)	C2-N2-Fe1	119.0(5)	C2-N2-Fe1	123.96(4)	C3-N3-Fe1	121.3(3)
C6-N2-Fe1	119.37(5)	C6-N2-Fe1	122.5(5)	C6-N2-Fe1	119.46(4)	C7-N3-Fe1	122.1(3)
C2-N2-C6	117.74(6)	C2-N2-C6	118.5(6)	C2-N2-C6	116.58(5)	N1-C1-Pd1	174.8(4)
N1-C1-Pt1	176.07(4)	N1-C1-Pt1	176.6(4)	N1-C1-Pd1	175.32(3)	N2-C2-Pd1	173.4(4)
C4-C7-N3	112.97(8)	C4-C7-N3	113.4(7)	C4-C7-N3	116.02(6)	C5-C8-N4	112.6(6)
C4-C7-O1	121.61(8)	C4-C7-O1	121.6(7)	C4-C7-O1	121.41(7)	C5-C8-O1	124.2(6)

Symmetry codes: **1**·4.5H_2O-c at 296 K: i) 1-*x*, *y*, 1-*z*; ii) *x*, 1-*y*, *z*; iii) 1+*x*, 1+*y*, *z*; iv) 1+*x*, *y*, *z*-1; 100 K: i) 1-*x*, *y*, -*z*; ii) *x*, -*y*, *z*; iii) 1+*x*, 1+*y*, *z*; iv) *x*-1, *y* 1+*z*; **2**·4.5H_2O-c at 296 K: i) -*x*, *y*, 1-*z*; ii) *x*, 1-*y*, *z*; iii) 1+*x*, 1+*y*, *z*; iv) 1+*x*, *y*, *z*-1; 100 K: i) 1-*x*, *y*, 1/2-*z*; ii) *x*, 1+*y*, *z*; iii) 1+*x*, *y*, *z*; iv) 1-*x*, 2-*y*, -*z*.

Table S2 Hydrogen-bond geometry (Å, °) for **1**·4.5H_2O-c and **2**·4.5H_2O-c at 296 and 100 K

D–H···A	d(D–H)	d(H···A)	d(D···A)	∠D–H···A
		1·4.5H_2O-c (296 K)		
C5–H5···O1^{i}	0.93	2.45	3.351(7)	164
N3–H3···O1W^{ii}	0.90	1.91	2.757(7)	156
O1W–H1WA···O2WA	0.85	2.54	3.357(4)	163
O1W–H1WB···O1^{i}	0.85	2.15	2.987(5)	169
O1WA–H1WD···O2WA	0.85	1.84	2.603(9)	148
O2W–H2WA···O1W^{ii}	0.85	1.99	2.629(6)	131
		1·4.5H_2O-c (100 K)		
C3–H3···O1^{i}	0.93	2.46	3.358(6)	164
N3–H3A···O1W^{iii}	0.90	1.94	2.772(2)	153
O2W–H2WA···O1^{iv}	0.85	1.83	2.669(2)	171
O2W–H2WB···O1W^{ii}	0.85	2.01	2.847(2)	171
O1W···O3W			2.695(3)	
		2·4.5H_2O-c (296 K)		
C5–H5···O1^{i}	0.93	2.45	3.357(13)	164
N3–H3···O1W	0.90	1.92	2.777(6)	158
O1W–H1WA···O1^{ii}	0.85	2.43	3.017(4)	127
O1W–H1WB···O2W^{ii}	0.85	2.59	3.151(5)	124
O2W–H2WA···O1	0.85	1.70	2.52(5)	162
		2·4.5H_2O-c (100 K)		
N4–H4···O1W	0.89	2.18	2.784(7)	124
O3W–H3WB···O1W^{ii}	0.85	1.71	2.562(6)	177
O3W–H3WA···O1	0.85	2.08	2.926(6)	176
C6–H6···O1^{i}	0.95	2.54	3.447(3)	161
O1W–H1WB···O4W^{iii}	0.85	1.95	2.529(6)	125

O2W···O4W	2.457(2)
O4W···O3W	2.595(7)

Symmetry codes: **1**·4.5H_2O-c at 296 K: i) 1-*x*, 1-*y*, -*z*; ii) 1+*x*, *y*, *z*; at 100 K: i) 1-*x*, -*y*, 1-*z*; ii) 1-*x*, *y*, 1-*z*; iii) -*x*, 1-*y*, 1-*z*; iv) *x*, 1+*y*, *z*. **2**·4.5H_2O-c at 296 K: i) -*x*, *y*, -*z*; ii) 1-*x*, 1-*y*, -*z*; at 100 K: i) 2-*x*, 1-*y*, 1-*z*; ii) *x*, 1-*y*, 0.5+*z*; iii) *x*, 1+*y*, *z*.

7. Second magnetic measurements for the hysteretic SCO behaviors of 1·4.5H_2O-c and 2·4.5H_2O-c

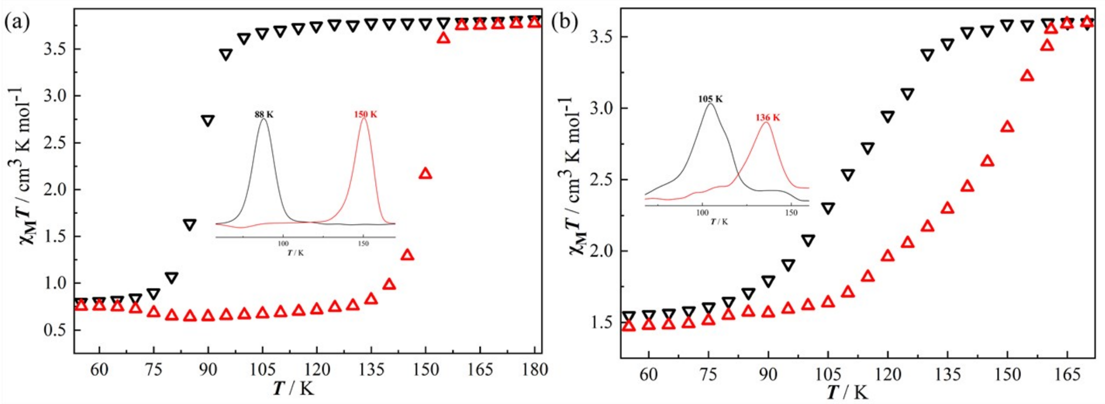

Fig. S15 Variable temperature magnetic susceptibility ($\chi_M T$) for (a) **1**·4.5H_2O-c and (b) **2**·4.5H_2O-c measured again in the range of hysteresis loop (black: cooling; red: heating; inset: $\partial(\chi_M T)/\partial T$ showing the $T_{1/2}$ values).

8. Comparison of the spin transition parameters of some representative 3D Hofmann SCO frameworks

Table S3 Critical temperature ($T_{1/2}$) and hysteresis width (ΔT) of some representative 3D Hofmann SCO frameworks [FeLM(CN)$_4$]·G and [FeL{M′(CN)$_2$}$_2$]·G with the rigid pillars except bph (M = Ni, Pt, Pd; M′ = Ag, Au; L = pillar ligand; G = guest molecule)

L	M	G	$T_{1/2}\downarrow$ (K)	$T_{1/2}\uparrow$(K)	ΔT (K)	Ref.
bpe	Ag		120	215	95	1
dpb	Au	0.7naphthalene	141	214	73	2
pz	Pt	0.5thiourea	213	277	64	3
bph	Pt	4.5H_2O	90(88)	150	60(62)*	this work
bpac	Pt	0.5bpac	251	300	49	4
bpy	Ni	*x*$(CD_3)_2CO$	103	148	45	5
pz	Pd	2.5H_2O	233	266	33	6
bpac	Pd	0.5bpac	283	315	32	4
bph	Pd	4.5H_2O	105	135(136)	30(31)*	this work
bpb	Pt	nitrobenzene	210	237	27	7
pz	Ni	2H_2O	280	305	25	6
2,5-bpp	Au	*s*BuOH	186/171	209/189	23/18	8
azpy	Pd		181	202	21	9
bpac	Pt	H_2O·0.5bpac	301	322	21	4
bpd	Au		158/128	179/149	21/21	10
pz	Pt	2H_2O	220	240	20	6
bpan	Au		242/143	252/163	10/20	11
4-abpt	Ag	*x*EtOH	264	281	17	12

azpy	Pt		175	190	15	9
dpe	Pt	0.5dpe	135	150	15	13
bpn	Ag	azobenzene	182/171/132/118	184/177/147/128	2/6/15/10	14
azpy	Pt	H_2O	275	285	10	9
azpy	Pd	H_2O	287	296	9	9
dpoda	Ag	1.5naphthalene	250/228/190/181	252/232/194/187	2/4/4/6	15
dpt	Pt	$1.5H_2O\cdot$dpt	210/127	212/132	2/5	16
Hbpt	Pt	0.5Hbpt·0.5MeOH·$2.5H_2O$	244/158/124	249/158/124	5/0/0	17
bipytz	Au		273	277	4	18
bpac	Pd	$H_2O\cdot$0.5bpac	307	310	3	4
dpe	Pt	$H_2O\cdot$0.5dpe	275/243	275/243	0/0	13
dpni	Ag	$4CH_3CN$	196/160	196/160	0/0	19

* The data were obtained from the second magnetic measurements.

References

1 V. Niel, M. C. Muñoz, A. B. Gaspar, A. Galet, G. Levchenko and J. A. Real, *Chem. Eur. J.*, 2002, **8**, 2446-2453.

2 J.-Y. Li, C.-T. He, Y.-C. Chen, Z.-M. Zhang, W. Liu, Z.-P. Ni and M.-L. Tong, *J. Mater. Chem. C.,* 2015, **3**, 7830-7835.

3 F. J. M. Lara, A. B. Gaspar, D. Aravena, E. Ruiz, M. C. Muñoz, M. Ohba, R. Ohtani, S. Kitagawa and J. A. Real, *Chem. Commun.*, 2012, **48**, 4686-4688.

4 C. Bartual-Murgui, N. A. Ortega-Villar, H. J. Shepherd, M. C. Muñoz, L. Salmon, G. Molnár, A. Bousseksou and J. A. Real, *J. Mater. Chem.*, 2011, **21**, 7217-7222.

5 K. Hosoya, S. Nishikiori, M. Takahashi and T. Kitazawa, *Magnetochemistry*, 2016, **2**, 8.

6 V. Niel, J. M. Martinez-Agudo, M. C. Muñoz, A. B. Gaspar and J. A. Real, *Inorg. Chem.*, 2001, **40**, 3838-3839.

7 L. Piñeiro-López, M. Seredyuk, M. C. Muñoz and J. A. Real, *Chem. Commun.*, 2014, **50**, 1833-1835.

8 J.-Y. Li, Y.-C. Chen, Z.-M. Zhang, W. Liu, Z.-P. Ni and M.-L. Tong, *Chem. Eur. J.*, 2015, **21**, 1645-1651.

9 G. Agustí, S. Cobo, A. B. Gaspar, G. Molnár, N. O. Moussa, P. A. Szilágyi, V. Pálfi, C. Vieu, M. C. Muñoz, J. A. Real and A. Bousseksou, *Chem. Mater.*, 2008, **20**, 6721-6732.

10 H.-T. Xu, Z.-L. Xu and O. Sato, *Microporous Mesoporous Mater.*, 2014, **197**, 72-76.

11 M. Meneses-Sánchez, L. Piñeiro-López, T. Delgado, C. Bartual-Murgui, M. C.

Muñoz, C. P. Chakraborty and J. A. Real, *J. Mater. Chem. C.*, 2020, **8**, 1623-1633.
12 W. Liu, Y.-Y. Peng, S.-G. Wu, Y.-C. Chen, M. N. Hoque, Z.-P. Ni, X.-M. Chen and M.-L. Tong, *Angew. Chem. Int. Ed.*, 2017, **56**, 14982-14986.
13 F. J. M. Lara, A. B. Gaspar, M. C. Muñoz, M. Arai, S. Kitagawa, M. Ohba and J. A. Real, *Chem. Eur. J.*, 2012, **18**, 8013-8018.
14 K.-P. Xie, Z.-Y. Ruan, B.-H. Lyu, X.-X. Chen, X.-W. Zhang, G.-Z. Huang, Y.-C. Chen, Z.-P. Ni and M.-L. Tong, *Angew. Chem. Int. Ed.*, 2021, **60**, 27144-27150.
15 C.-J. Zhang, K.-T. Lian, G.-Z. Huang, S. Bala, Z.-P. Ni and M.-L. Tong, *Chem. Commun.*, 2019, **55**, 11033-11036.
16 K.-T. Lian, W.-W. Wu, G.-Z. Huang, Y. Liu, S.-G. Wu, Z.-P. Ni and M.-L. Tong, *Inorg. Chem. Front.*, 2021, **8**, 4334-4340.
17 F.-L. Liu, D. Li, L.-J. Su and J. Tao, *Dalton Trans.*, 2018, **47**, 1407-1411.
18 J. E. Clements, J. R. Price, S. M. Neville and C. J. Kepert, *Angew. Chem. Int. Ed.*, 2014, **53**, 10164-10168.
19 Y. Meng, Y.-J. Dong, Z. Yan, Y.-C. Chen, X.-W. Song, Q.-W. Li, C.-L. Zhang, Z.-P. Ni and M.-L. Tong, *Cryst. Growth. Des.*, 2018, **18**, 5214-5219.